JTTEE5 17:124–135
DOI: 10.1007/s11666-007-9141-5
1059-9630/$19.00 © ASM International

Peer Reviewed

Thermal Barrier Coatings Made by the Solution Precursor Plasma Spray Process

Maurice Gell, Eric H. Jordan, Matthew Teicholz, Baki M. Cetegen, Nitin P. Padture, Liangde Xie, Dianying Chen, Xinqing Ma, and Jeffrey Roth

(Submitted February 6, 2007; in revised form August 18, 2007)

The solution precursor plasma spray (SPPS) process is a relatively new and flexible thermal spray process that can produce a wide variety of novel materials, including some with superior properties. The SPPS process involves injecting atomized droplets of a precursor solution into the plasma. The properties of resultant deposits depend on the time-temperature history of the droplets in the plasma, ranging from ultra-fine splats to unmelted crystalline particles to unpyrolized particles. By controlling the volume fraction of these three different constituents, a variety of coatings can be produced, all with a nanograin size. In this article, we will be reviewing research related to thermal barrier coatings, emphasizing the processing conditions necessary to obtain a range of microstructures and associated properties. The SPPS process produces a unique strain-tolerant, low-thermal conductivity microstructure consisting of (i) three-dimensional micrometer and nanometer pores, (ii) through-coating thickness (vertical) cracks, (iii) ultra-fine splats, and (iv) inter-pass boundaries. Both thin (0.12 mm) and thick (4 mm) coatings have been fabricated. The volume fraction of porosity can be varied from 10% to 40% while retaining the characteristic microstructure of vertical cracks and ultra-fine splats. The mechanism of vertical crack formation will be described.

Keywords plasma spray, solution precursor, solution precursor plasma spray, thermal barrier coatings

1. Introduction

1.1 Thermal Spray

The application of metallic and ceramic coatings using thermal processes has been commercially employed for decades. Current methods include electron beam physical vapor deposition (EB-PVD), high-velocity oxygen fuel (HVOF), air plasma spray (APS), and vacuum plasma spray (VPS). The deposition of coatings using a plasma spray process is one of the most popular commercial methods, with an annual global market of nearly five billion dollars (Ref 1). The standard approach involves feeding fine powder into a plasma jet, where it is melted and subsequently deposited onto a substrate.

It is widely recognized that deposition of small, melted particles achieves a fine microstructure, which in turn leads to improvements in certain desirable mechanical properties such as strength and hardness. Unfortunately, it is generally not possible to feed powders finer than 5-10 μm due to the effects of surface forces on powder flow. Recently, the suspension plasma spray process (SPS) was developed, in part to overcome this limitation (Ref 2-4). In this process, nano-sized particles are suspended in a liquid before injection into the plasma plume, circumventing normal feeding problems.

This article will examine a relatively new technology, the solution precursor plasma spray (SPPS) and its use in a specific advanced application: thermal barrier coatings (TBCs). Similar to existing plasma deposition methods, the SPPS process deposits melted feedstock material onto a substrate as 'splats.' However, the primary differentiating attribute between SPPS and other methods is that the feedstock material is in the form of a liquid solution rather than a powder or a powder suspension. As a result, the SPPS process is able to deliver fine splats without the difficulties and limitations of both fabricating and feeding fine solid powders. Instead, SPPS has the challenge of formulating high-molarity solutions and engineering their chemical and physical properties.

Although this review will concentrate specifically on the SPPS process for making TBCs, the process is more generally versatile. Some attributes that make it amenable to a wide variety of applications are listed below:

(i) Since the process uses precursor solutions, molecular level mixing of constituent chemicals results in chemical homogeneity. The SPPS process also allows for the possibility of creating metastable coating

Maurice Gell, Eric H. Jordan, Matthew Teicholz, Baki M. Cetegen, and **Dianying Chen,** Department of Materials Science and Engineering, Institute of Materials Science, University of Connecticut, Storrs, CT; **Nitin P. Padture**, Department of Materials Science and Engineering, Ohio State University, Columbus, OH; **Liangde Xie**, Chromalloy Gas Turbine Corporation, San Antonio, TX; and **Xinqing Ma** and **Jeffrey Roth**, Inframat Corporation, Farmington, CT. Contact e-mail: mgell@mail.ims.uconn.edu

phases due to rapid cooling of ultra-fine splats during deposition (Ref 5, 6).

(ii) The chemical mixing of solutions also allows new precursor compositions to be quickly formulated and deposited as coatings. Multi-component coatings are easily made by combining liquid precursors in the appropriate proportions. This compares to other plasma spray processes where sprayable powders of each composition must be fabricated and then homogeneously combined.

(iii) By controlling the injection process, the amount of unpyrolized material can be modulated. This allows for deliberate deposition of semi-pyrolized material in some applications (such as TBCs, where it causes the formation of beneficial vertical cracking) while in other applications unpyrolized material can be eliminated (resulting in dense coatings consisting of ultra-fine splats.)

The solution precursor process was initially explored as a coating technology by Karthikeyan et al. (Ref 7-9). While demonstrating that the method was feasible, quality coatings could not be generated. SPPS material systems were first reported in 2001 (Ref 10-12) and in the 6 years since, extensive research on deposition mechanisms and coating properties has been conducted by the University of Connecticut (UConn) and Inframat Corporation collaborative research group (Ref 12-36).

Due to the unique technology that SPPS affords, resultant coatings offer a diverse spectrum of possible applications with coating properties controllable via spray and processing conditions. This review article will focus on the SPPS technology that is most highly developed: TBCs.

1.2 Thermal Barrier Coatings

Thermal barrier coatings are multi-layered material systems designed to insulate metallic components employed in hot sections of gas turbine engines (Ref 14, 37). Due to the nature of the operating environment, a successful TBC must be able to endure severe cyclic heating and the difference in the coefficient of thermal expansion (CTE) between the ceramic topcoat and the metallic substrate causes severe strains during these cyclic heating events. Additionally, within the commercial sector, cost is a critical metric.

The SPPS method lends itself particularly well to the development of new TBCs. The unique coating microstructure created by SPPS offers:

(i) Lower thermal conductivity than EB-PVD coatings and comparable thermal conductivity to the very best APS coatings. (~1.5 W/mK for EB-PVD, ~0.8 W/mK for APS, ~1 for SPPS (Ref 19))

(ii) Comparable, or in some cases higher, durability than APS and EB-PVD coatings. (2.5× compared to APS, 1.5× compared to EB-PVD (Ref 20, 25-27))

(iii) Costs comparable to APS coatings and lower than EB-PVD coatings.

2. The SPPS Process

The SPPS coating system consists of a pressurized liquid reservoir from which the chemical solution is injected into the plasma plume. Figure 1 shows this schematically

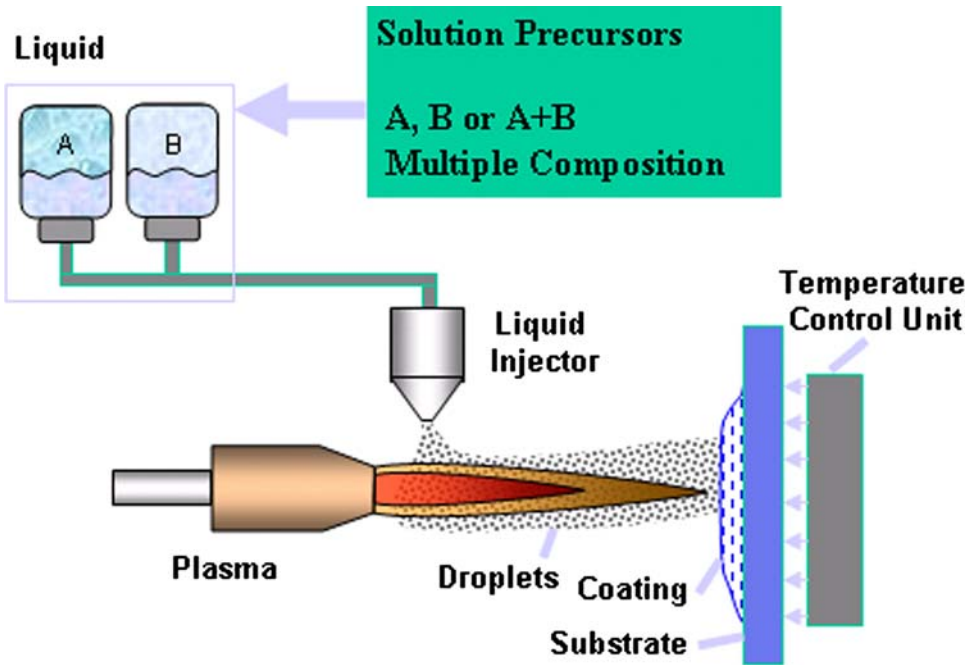

Fig. 1 Schematic of the solution precursor plasma spray delivery system

where injection takes place outside of the nozzle using an atomizing injector. The precursor consists of an aqueous solution of zirconium and yttrium salts (Inframat Corp, Farmington, CT) and, in the present case, the plasma jet is generated by a direct current 9 MB plasma torch (Sulzer Metco, Westbury, NY) attached to a six-axis robotic arm. Operating power ranges from 35 to 45 kW, with argon as the primary gas and hydrogen as the secondary gas. Injection pressurization is accomplished with nitrogen.

2.1 Deposition Mechanisms

The plasma plume into which the liquid precursor is injected can be divided into three main regions: (i) a cold temperature region on the periphery, (ii) a moderate temperature area around this inner core, and finally (iii) the hot inner core. These regions are shown schematically in Fig. 2.

The droplet momentum and injection location determine which area of the plasma plume that a droplet will entrain and this in turn determines the thermal, or time-temperature, history of that droplet. This is shown schematically in Fig. 3. Since the chemical and physical processes that a droplet undergoes are dependent on the heating that it experiences, the deposition state of the coating is a direct function of this thermal history.

Once entrained, a droplet undergoes some or all of the following processes depending on the amount of heat transferred to it from the plasma: precursor solvent evaporation, droplet breakup, precursor solute precipitation, pyrolysis, sintering, melting, and crystallization. These processes are shown in Fig. 4. Droplets may deposit onto the substrate after undergoing some or all of theses processes.

Previous work has aimed to identify deposition mechanisms by investigating droplets inside the plasma plume (via impact sampling), high and normal speed single scans onto substrates, shielded spraying that isolate regions of the plume, and stationary torch experiments with a high-speed moving substrates (Ref 13, 15, 24, 26). Each of these experiments sought to either isolate some spatial region of the plume or some temporal section of the process from which a more complete picture of deposition could be established. As a result of this experimentation, a relationship between the droplet trajectory and the resulting deposit microstructure has been established.

The following five deposition mechanisms have been identified:

(i) Droplets that entrain in the hot inner core of the plasma plume experience the most heating and exhibit mechanisms, A, B, and C, shown in Fig. 4, eventually depositing as melted material. Given a known injected droplet size, it has been observed that arriving droplets are smaller than predicted by simple mass balance leading to the conclusion that some breakup process occurs after the droplet has been injected. This breakup is discussed in later sections of this article. The smaller droplets then undergo further heating to a fully melted state and crystallize on impact to form ultra-fine (0.5-2 μm) splats seen in Fig. 5(a). This is the primary deposition mode for SPPS (Ref 15, 24, 26, 27).

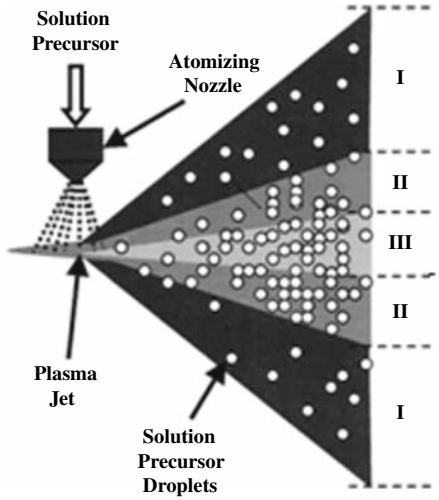

Fig. 2 Regions of the plasma plume. (I) cold outer region, (II) moderate inner core, and (III) the hot inner core

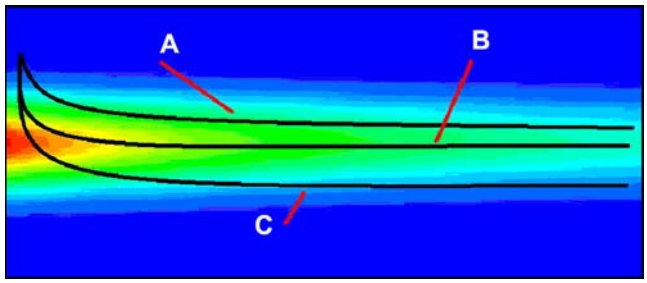

Fig. 3 Possible trajectories of a droplet injected into the plasma plume. (A) underpenetration, (B) ideal penetration, and (C) overpenetration

(ii) At certain torch stand off distances, droplets will undergo all mechanisms shown in Fig. 4(a-d), re-solidifying and crystallizing before impact with the substrate to form fine crystalline spheres (Fig. 5b). These spheres adhere in small fractions to the substrate after being captured by gel or softer deposit phases and are a very small fraction of total deposit volume (Ref 15, 26).

(iii) Droplets can also be entrained in the cold region of the plasma plume and undergo processes shown in box (a) in Fig. 4. Here, droplets experience sufficient heating to cause solute evaporation leading to the formation of a gel phase, which deposits on the substrate. Alternatively, some cold region droplets form a pyrolized shell containing unpyrolized solution. These droplets then fracture during deposition (Fig. 5c) (Ref 24, 26, 31, 34).

(iv) Some precursor solution can arrive at the substrate in liquid form, having undergone none of the processes shown in Fig. 4. This deposition method can be largely eliminated by spray parameters.

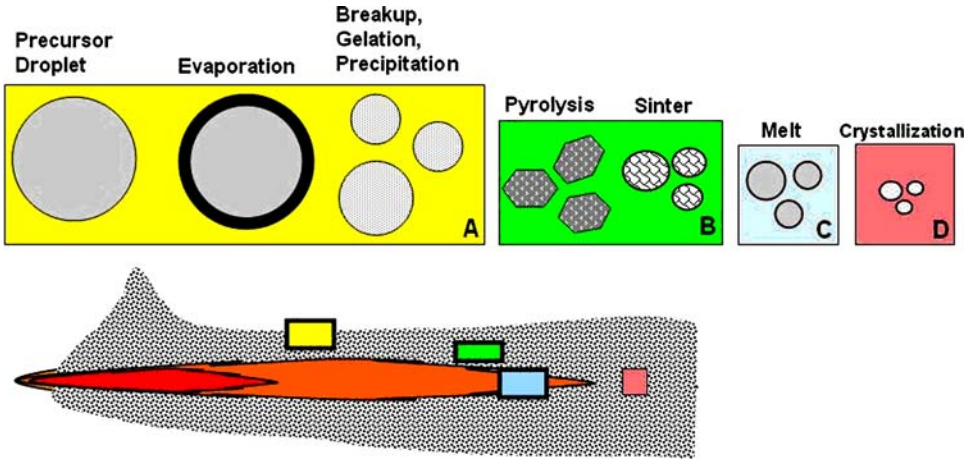

Fig. 4 Chemical and physical evolution of a droplet injected into the plasma plume

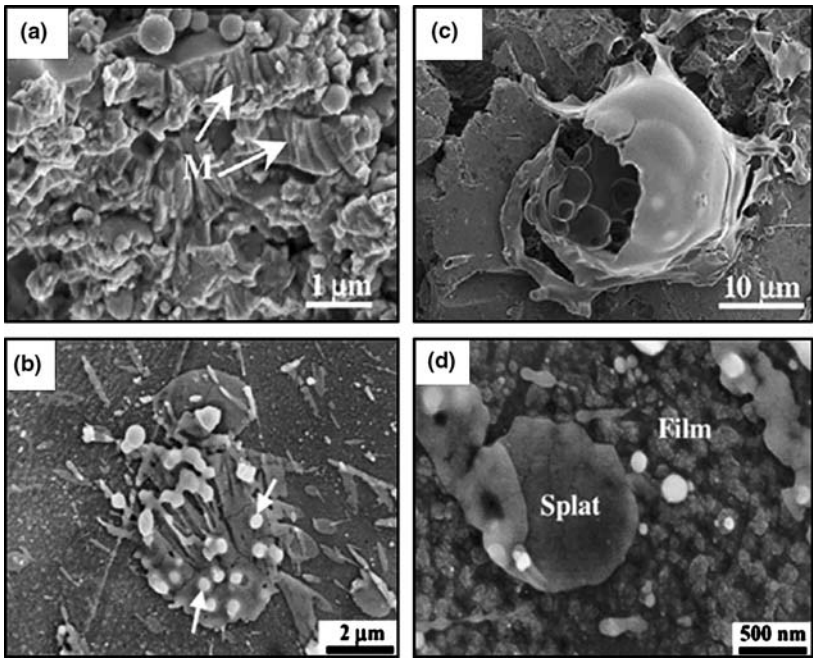

Fig. 5 Several deposition modes of SPPS. (a) Fine splats, (b) crystallized spheres, (c) ruptured shell, and (d) vapor deposited film

(v) Precursor has also been found to reach the substrate as a vapor deposited thin film (Fig. 5d). This film has not been found in coatings (it was instead discovered during a high-speed single pass experiment), but this may be to due to its small relative feature size (100 nm compared to <2 μm splats). These deposits are very small fraction of the total deposit volume (Ref 26).

It is possible to control each of the deposition mechanisms, and hence the coating microstructure. The porosity level, density, hardness, and vertical cracking can be altered by spray parameters such as plume temperature, plume velocity, injection location, injection velocity, droplet size, standoff distance, and substrate temperatures. These parameters were systematically studied in model spray experiments (Ref 13, 24, 34). Xie et al. found that the plume penetration depth of liquid precursor was governed by droplet momentum and plasma plume momentum at the injection location. By holding the plume at constant conditions, droplet penetration depth could be varied by changes in solution feed rate and atomizing pressure. This penetration depth was correlated to the location of adherent substrate deposits and the deposition efficiency (Ref 24).

2.2 Liquid Injection

In the SPPS process, it is desirable to control both the size and melt state of the delivered splats. While the splat sizes depend primarily on the molarity of precursor solution and final droplet size, the degree of melting depends on the droplet trajectory and injection location.

When making TBCs, it is desirable to have a controlled fraction of the injected liquid entrained in the cooler periphery region of the jet in order to deliver semi-pyrolized material to the substrate. As will be discussed in later sections, this unpyrolized material is critical to the formation of vertical cracks. The TBCs discussed in this article were produced using a transverse air blast cone spray atomizer. This atomizer delivers a cone pattern distributing spray over a region of the plasma jet, entraining some in the hot inner core and some in the colder regions of the plume. This enables the deposition of unpyrolized material in a regulated manner. Droplet sizes determined by Phase Doppler Particle Aanemometry (PDPA) range from 1 to 100 μm with an average size of 40 μm and a standard deviation of approximately 5 μm (Ref 18).

Part of the flexibility that the SPPS process offers is based on the potential control of liquid injection. For example, dense coatings, where no unpyrolized material is desired, require different injection techniques than TBCs. The best results to date for dense coatings have been achieved by custom made capillary atomizers and direct stream injection using the plasma itself as the atomizing gas. The custom made atomizer consisted of two capillary tubes, one carrying atomizing gas and mounted redial to the jet center line and another carrying solution precursor mounted circumferential to the jet axis. With its influence on droplet entrainment, injection technology is an area of active research.

2.3 Droplet Formation

The behavior of droplets after injection is not yet fully understood, due in large part to the hostile environment and small particle sizes that make direct observation very difficult. By simple mass balance, if no breakup process occurs, splat sizes on the substrate would have a mean size of approximately 5-10 μm. However, as previously mentioned, observed splats are found to be 0.5-2 μm. Additionally, the size of the droplets required to make the observed splat sizes 0.5-2 μm have been shown in simulation to be too small to entrain in the hot core of the plasma jet and the population of those droplets are not sufficient to explain the observed deposition rates. Clearly, post-injection droplet breakup occurs.

Extensive modeling efforts have provided insight into how this occurs, including, but not limited to, the possible breakup mechanisms described below (Ref 18, 30-34).

2.3.1 Aerodynamic. The injection of solution into the plasma plume and subsequent potential breakup processes are highly dependent on the relative velocities experienced by injected droplets. For most applications, aerodynamic droplet breakup should be avoided as it can cause uncontrolled final droplet sizes. The tendency for aerodynamic breakup is given to a first-order by the Weber number

$$\mathrm{We} = \frac{\rho v^2 l}{\sigma}$$

where ρ is the fluid density, v the relative velocity, l the characteristic length, and σ the fluid surface tension. Modeling has shown that for nominal plasma plume velocities of the 9 MB gun used here, droplets smaller than 50 μm will not undergo aerodynamic breakup. Thus, the post-injection breakup cannot be explained by these forces.

However, since aerodynamic breakup is a direct function of the relative velocity experienced by the droplet, consideration has been given to the effects of plasma plume arc root fluctuations. Moreau (Ref 38) has shown that localized particle velocities can vary by as much as 30% due to these arc fluctuations. However, the magnitude of these variations are significantly less than the magnitude of the velocity difference at the instant of injection. In other words, despite any velocity variation, if aerodynamic breakup is to occur, it will do so immediately after being injected, not because of later arc root fluctuation induced velocity changes.

There is the case, however, that two droplets may be injected into the plasma and experience two different plume velocities. If the extreme case is considered, where one droplet enters at the peak of a velocity cycle and another at the trough, minimum size for undesirable aerodynamic breakup will likewise be at two different sizes. Since the high-velocity (cycle peak) case will be the limiting factor in injection capabilities (the need to inject a smaller droplet to preclude breakup), modeling has shown that given a 2× velocity increase, the maximum droplet size would have to be 33 μm.

Thus, another non-aerodynamic breakup process must operate. This process is believed to be related to the series of physical states the droplet undergoes due to chemical and physical changes associated with heating. The following sections give the current state of understanding of this stage of the SPPS process.

2.3.2 Sphere Rupture. Additional investigation concentrated on the selective surface solvent loss and formation of solid shells that was mentioned earlier in this article. The formation of these shells has been modeled, observed in laser heating experiments, and as actual deposited material (Fig. 5c). These shells of concentrated precursor are believed to lead to pressurization and rupture, resulting in smaller droplets. This method of breakup depends greatly on the gas permeability of the precursor gel and solute shell and is believed to be one of the primary breakup mechanism for droplets smaller than 40-50 μm.

2.3.3 Shedding. In other cases utilizing aluminum precursors, the droplet surface was observed to detach from the droplet core during laser heating experiments. The process of shedding is not yet understood and is still under investigation.

Despite extensive modeling efforts, complete understanding of the droplet breakup processes at the high-heating rates relevant to the SPPS process is not yet available. However, some additional insight may be obtained from spray pyrolysis literature (Ref 39-43).

3. Results

Certain performance characteristics of SPPS deposited TBCs are a direct result of unique microstructural features.

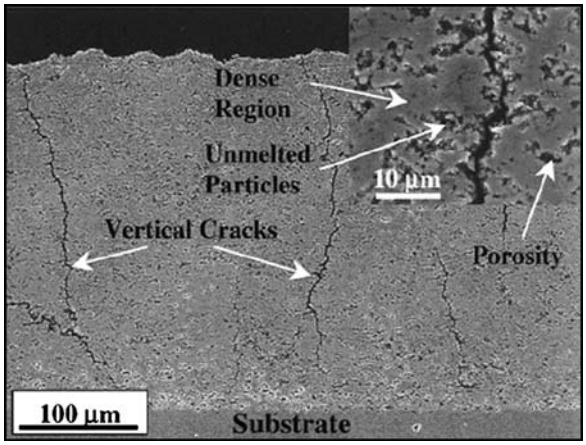

Fig. 6 Features of SPPS TBCs, including vertical cracks, dense regions of ultra-fine splats, small and uniformly dispersed porosity, and unmelted particles

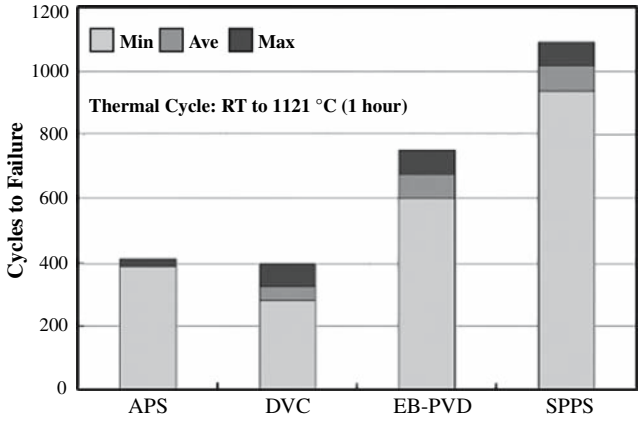

Fig. 7 Cyclic durability comparison of APS, DVC, EB-PVD, and SPPS TBCs for 1 h cycles at 1121 °C

These features include: ultra-fine splats (which form dense coating regions), through thickness vertical cracks, embedded unpyrolized particles, and porosity. These features are shown in Fig. 6.

3.1 Bond Strength

As with APS, splats are created when molten feedstock impacts the substrate. However, the creation of ultra-fine splats by SPPS imparts increased bond strength and durability compared to the large-scale splats characteristic of APS coatings. When deposited onto mild steel substrates and tested by specifications set forth in ASTM 633, the bond strength of conventional APS deposited coatings was found to be 19.9 MPa, while the bond strength of SPPS coatings was 22% higher, at 24.2 MPa (Ref 27).

The improved bond strength is probably a direct result of the finer splat size, as SPPS deposited splats experience more uniform cooling due the increased surface area to volume ratio. Larger APS splats, with an area 2500× that of SPPS, experience non-uniform cooling and can become distorted during the process, resulting in poorer bonding with the underlying splats. The improved bonding in SPPS TBCs leads to increased resistance to splat boundary crack initiation and propagation compared to APS TBCs.

3.2 Vertical Cracks

Vertical cracks in TBCs are known to increase the coating's ability to tolerate the thermal strain generated during thermal cycling (Ref 37). The vertical cracks found in SPPS coatings form by the pyrolysis and subsequent volume shrinkage of un-decomposed precursor embedded in the coating during deposition. The amount of un-decomposed precursor can be controlled by spray parameters, primarily droplet injection momentum and the formation of these cracks can be controlled by heat exposure, either by plasma torch passes or post-processing treatment (Ref 20). Additional support for this explanation of the formation of vertical cracking is found in dense coatings also made by the SPPS process. In these coatings, unpyrolized material is deliberately eliminated as a deposit, and subsequently no vertical cracking appears.

It should be noted that the formation mechanism of these vertical cracks is different than those obtained in dense vertically cracked (DVC) APS TBCs. Developed by Taylor (Ref 44), DVC coatings form vertical cracks during deposition by the thermal stress of repeated coating layers, followed by subsequent cooling, and occur only in coatings with of 88% density or higher. The durability and failure mechanisms of these coatings have been reviewed elsewhere (Ref 23).

3.3 TBC Cyclic Durability

Vertical cracking, along with improved bonding, and higher in-plane fracture toughness increase the coating's cyclic durability in the thermal cycling environments experienced by TBCs. The durability of SPPS TBC samples was tested using a bottom loading, custom designed, automated furnace (CM Inc., Bloomfield, NJ). Samples were mechanically lifted into the furnace chamber and brought to 1121 °C during a 10-min ramp up. After soaking at the programmed temperature, the samples are lowered and air quenched by an electric fan. Temperature control was accomplished using a thermocouple welded to a dummy disc sample and a stand-alone data acquisition system recorded temperature throughout the cycle. Figure 7 shows the spallation lives of a number of production TBCs compared to SPPS TBCs. It can seen that SPPS TBCs have a 2.5× spallation life improvement compared to APS coatings on the same bond coat and substrate and an equivalent life advantage compared to production DVC coatings. UConn has tested at least six production EB-PVD TBCs and Fig. 7 represents the best obtained spallation life. SPPS TBCs exhibit a 1.5× improvement in life compared to very good EB-PVD TBCs (Ref 22, 27-29).

These favorable results for SPPS TBCs are seen when spallation occurs predominantly in the ceramic layer near the thermally grown oxide (TGO), a common failure mode for TBCs (Ref 14, 37). In these instances, the benefits of the vertical cracks and higher in-plane toughness

are manifest. With other bond coats, where spallation is predominantly in the TGO, at the ceramic/TGO, or TGO/bond coat interfaces, or mixtures of these spallation modes, the benefits of the vertical cracks are not realizable and SPPS TBCs exhibit equivalent lives to APS TBCs.

3.4 Thermal Conductivity

As with APS, the embedded porosity in SPPS TBCs provides for the critical thermal resistance required in TBCs. In APS coatings, this porosity is concentrated in splat boundaries in the planar direction, perpendicular to the heat flux across the ceramic. In SPPS coatings, the porosity is smaller (50-200 nm) and more uniformly dispersed.

The thermal conductivity, as measured by laser flash technique from 100 to 1000 °C, of SPPS coatings has been compared to coatings generated by both EB-PVD and APS. Normal SPPS TBC's have been found to have a thermal conductivity of approximately 1.0-1.2 W/mK. This value is lower than EB-PVD coatings, but higher than conventional APS coatings (see Fig. 8). The cause for this high conductivity (relative to APS coatings) is believed to be due to the increased internal contact area that results from the significantly finer microstructure and higher splat-to-splat contact area (Ref 10).

Two methods have been developed to lower the thermal conductivity of SPPS TBCs.

3.4.1 Layered SPPS. The microstructure of SPPS coatings can be engineered to provide layers of high porosity between layers of normal porosity (Fig. 9). This layering of porosity is achieved by optimal selection of raster scan step height during deposition. These high-porosity layers act in the same manner as the planar porosity found in APS coatings, but without the associated reduction in durability and have been shown to reduce the thermal conductivity to 0.75 W/mK. The results of detailed object orientated numerical modeling of the microstructure shown in Fig. 9 have matched experimental thermal conductivity results. This strongly supports the assertion that the reduction in thermal conductivity is a direct result of these engineered microstructures (Ref 19).

3.4.2 Multicomponent Coatings. Due to the rapid compositional exploration that is possible with solution mixing, novel precursor solutions that reduce coating conductivity (Fig. 8a) have been developed with relatively modest effort. These coatings were created by co-doping the precursor solution with rare earth oxides such as neodymium oxide and gadolinium oxide. These multicomponent coatings structures retain the nominal SPPS microstructure while reducing coating thermal conductivity to 0.55 W/mK, one of the lowest reported values for TBCs (Ref 29, 36).

3.5 Thermal Stability

The thermal cyclic stability of SPPS coatings was examined and found to show no significant microstructural or phase changes during 1,090 1-h cycles at 1121 °C. Two critical SPPS features, vertical cracks and ultra-fine splats, remained stable throughout the test (Ref 21).

More extensive non-cyclic, thermal stability work was conducted by Chen et al. (Ref 35). In that study, the thermal stability of both SPPS and APS coatings were compared in a temperature range of 1200-1500 °C. Despite having very different as-coated microstructures, APS and SPPS TBCs exhibited similar grain growths, density increases and hardness increases between 1200 and 1400 °C. Above 1400 °C, APS TBCs exhibited a faster rate of grain growth and transformation to the monoclinic phase. These effects initiated in SPPS TBCs at 1500 °C. Vertical cracks were retained or reformed, even after exposure to 1500 °C. Figure 10 shows grain coarsening as a function of temperature for SPPS TBCs.

3.6 Mechanical Properties

The mechanical properties of SPPS coatings have been tested and compared directly with APS coatings on

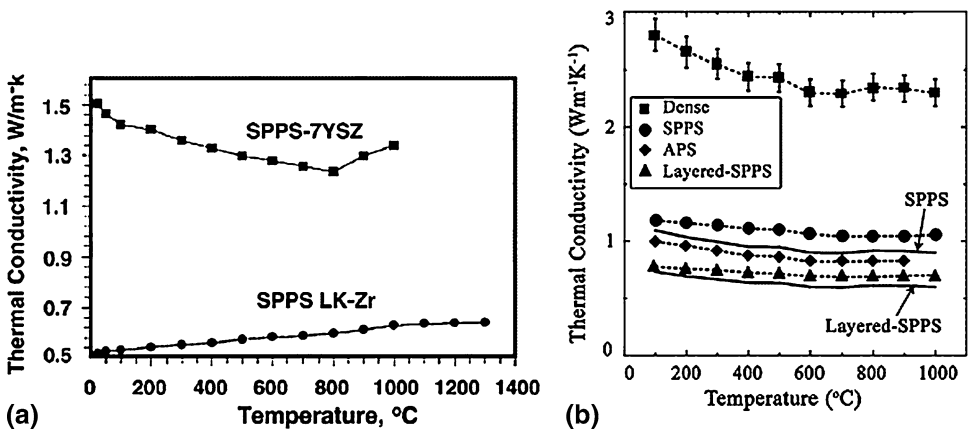

Fig. 8 (a) Thermal conductivity of advanced composition SPPS TBCs, (b) comparison of the thermal conductivity of SPPS, APS, and layered-SPPS coatings. Dense data represent the thermal conductivity of fully dense 7 wt.% YSZ

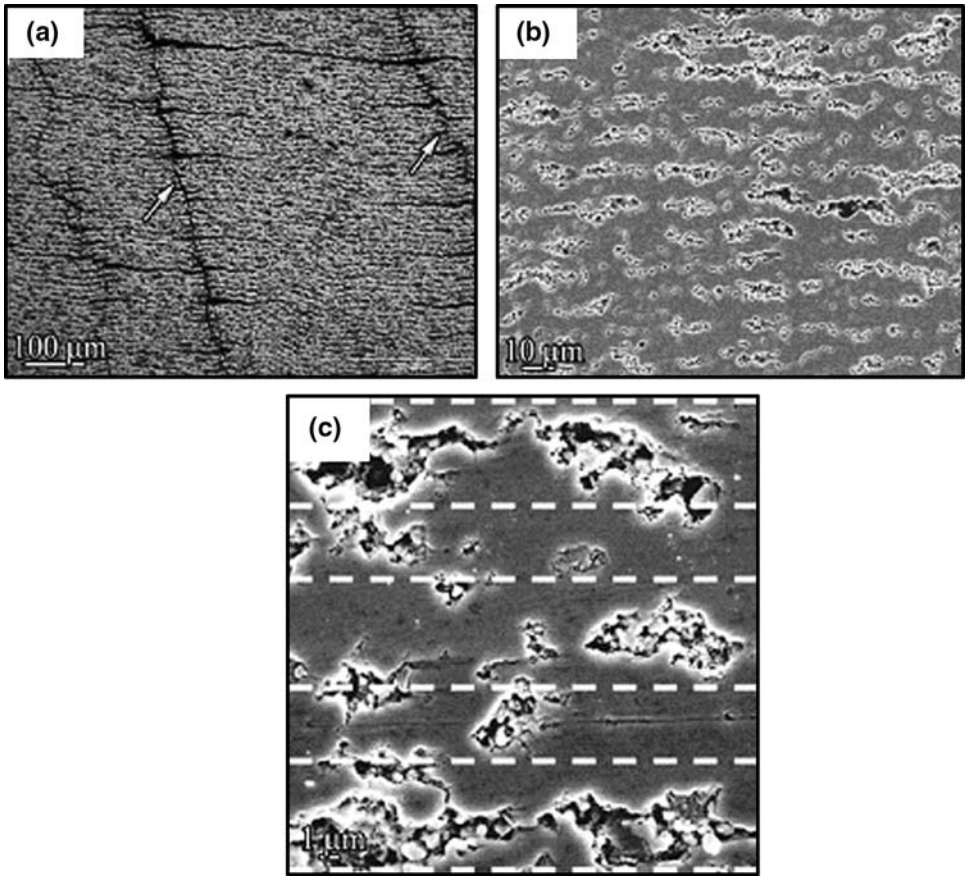

Fig. 9 Mictrostructure of layered SPPS coatings (a) low magnification, (b) higher magnification, (c) highest magnification-dashed lines approximately represent interpass boundaries

identical 304 stainless substrates (Ref 28). These values are shown in Table 1. Some features are notable. The difference between out of plane and in plane compressive strength of APS coatings vary by approximately 17% and elastic modulus by 5%. However, in SPPS coatings, the out of plane and in plane compressive strength and elastic modulus differ by 52% and 55%, respectively. Despite the isotropic nature of the porosity of SPPS coatings, it is apparent by this comparison that the SPPS vertical cracking has significant non-isotropic effects on certain mechanical properties.

3.7 Cost

SPPS technology is easily adapted to existing thermal spray systems. Additionally, the mixing and feeding of precursor solution is comparatively less intensive than the powder systems used in APS. The cost of SPPS coatings estimated by current practices and deposition efficiencies is significantly less costly than EB-PVD coatings and slightly higher in cost than APS coatings (Ref 29). This modest increase of cost for SPPS coatings compared to APS is the result of lower deposition rate. This is due to two primary causes: first, the need to evaporate solvent with some of the plasma jet enthalpy, and second, the need to embed some unpyrolized material into the coating (in the case of TBCs).

Since the main cost associated with lower deposition rates are operator costs, the overall cost differential between APS and SPPS deposition methods could be minimized by the use of larger, higher powered plasma guns such as Mettech Axial III, Metco Triplex, or Praxair Plazjet, where the Mettech gun has the added potential advantage of axial injection leading to better entrainment and more effective heating of the solution droplets.

3.8 Thick TBCs

It is also important to note that the microstructural features discussed in this section, which impart beneficial TBC qualities, are retained in very thick coatings. It is well known that the spallation life of APS coatings is markedly reduced with thickness due to the increase in stored strain energy (Ref 14, 37). However, with SPPS coatings, the spallation lives are significantly less thickness-sensitive and demonstrate superior lives as seen in

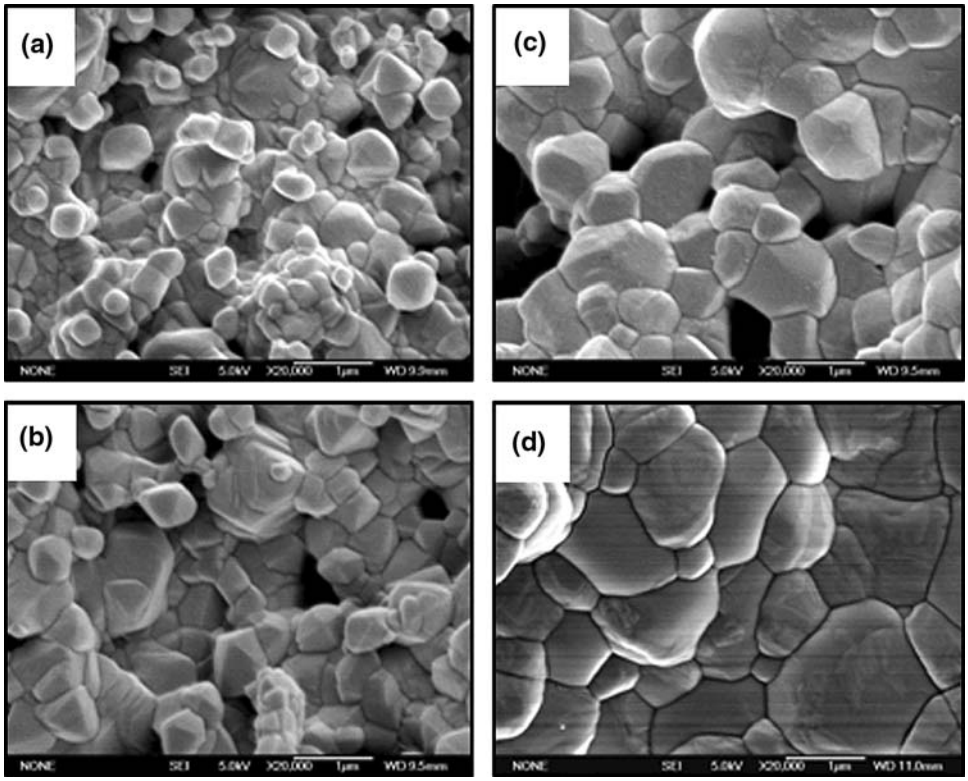

Fig. 10 Surface morphologies evolution as a function of heat treatment temperature (a) 1200 °C for 100 h, (b) 1300 °C for 100 h, (c) 1400 °C for 100 h, and (d) 1500 °C for 100 h

Table 1 Comparison of mechanical properties for TBCs generated by SPPS and APS (Ref 28)

	SPPS	APS
Indentation toughness		
In plane	1.7 MPa $m^{0.5}$	0.5 MPa $m^{0.5}$
Out of plane	1.2 MPa $m^{0.5}$	Cracks not well defined
Compressive strength		
In plane	540 (722-301) GPa	578 (648-423)
Out of plane	258 (306-190) GPa	476 (591-335)
Heat treated in plane	629 (697-504) GPa	Not tested
Elastic modulus		
In plane	49 (77-44) GPa	40 (47-35) GPa
Out of plane	22 (30-9) GPa	38 (41-32) GPa
Heat treated In plane	100 (122-71) GPa	Not tested
Secant modulus		
Cycle 1	3.1 GPa	10.3 GPa
Cycle 2	7.7 GPa	13.4 GPa
Cycle 3	13.6 GPa	17.3 GPa
Hardness	5.4 GPa	3.9 GPa

Fig. 8 (Ref 17, 28). Coatings up to 4 mm have been created on CMSX-4 substrates with APS-deposited NiCrAlY bond coats (Fig. 11). These coatings have demonstrated characteristic vertical cracking and low-thermal conductivity found in normal thickness (~250 μm) coatings while not suffering the same reduction in durability found in thick APS coatings (Fig. 12). These thicker coatings can be applied to combustors, stator vanes, and turbine abradable outer airseals and their potential is discussed in greater detail in Ref 17, 28.

4. Summary

The development of TBCs produced by the SPPS process has been reviewed.

- The SPPS method involves the injection of a precursor solution into a plasma plume, where the solution feedstock undergoes chemical and physical changes before being deposited on a substrate.
- The substitution of liquid feed over the powder feed results in:
  - (i) Rapid and complete mixing of precursor material
  - (ii) Precursor composition flexibility
  - (iii) Rapid screening of compositions
  - (iv) The creation of nano-structured coatings
  - (v) The creation of unique compositions, phases, and microstructures
- Current challenges of the SPPS method include:
  - (i) Precursor solution chemistry
  - (ii) Control over droplet entrainment
  - (iii) Control of deposit homogeneity

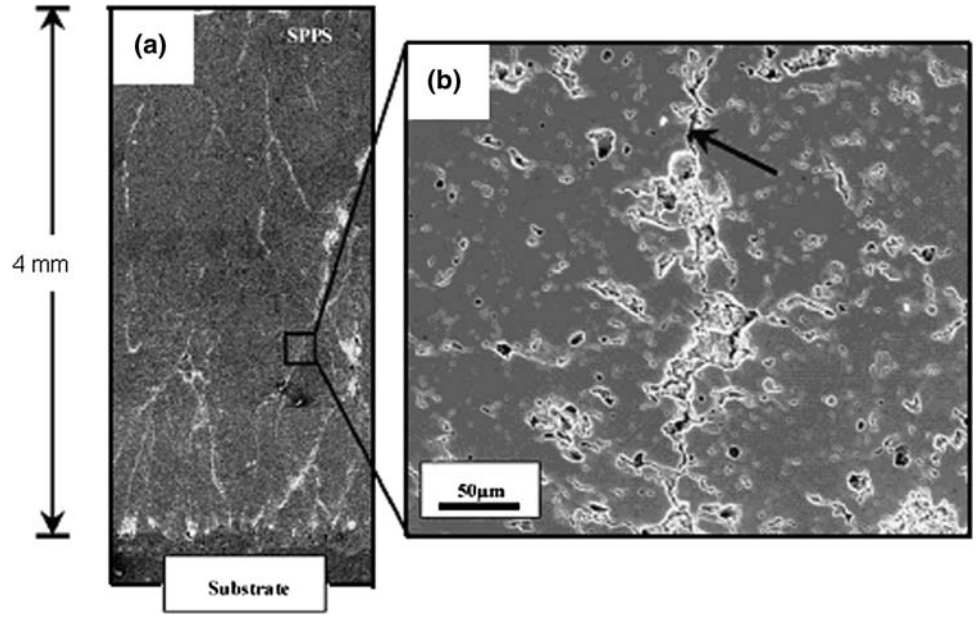

Fig. 11 Micrograph of thick SPPS sample (4 mm). (a) Low magnification, (b) higher magnification showing vertical cracking and retained microstructure

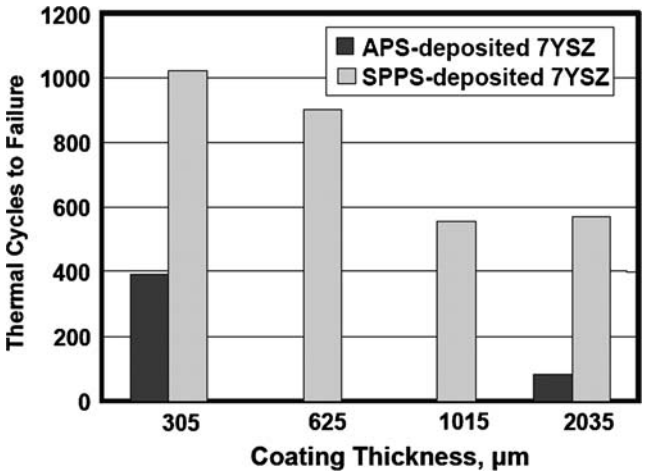

Fig. 12 Comparison of cyclic durability between SPS and APS coatings as a function of thickness

- The SPPS process lends itself particularly well to the creation of TBCs. By controlling injection parameters, it is possible to create a microstructure characterized by:

  (i) Strain relieving through thickness vertical cracks
  (ii) Fine, dispersed porosity
  (iii) Ultra-fine splats with enhanced splat-to-splat bonding

- The deposition state of SPPS coatings is a function of the thermal history of solution droplets. This history is in turn a function of droplet entrainment in the plasma plume and can be extensively varied through injection parameters such as gas pressures and feed rates.
- Compared to production TBCs, coatings produced by the SPPS process demonstrate:

  (i) Equal or greater durability
  (ii) Lower thermal conductivity
  (iii) Higher in-plane toughness and bond strength
  (iv) Lower costs than EB-PVD and comparable costs to APS

- The flexibility of the SPPS process can be used to create durable TBCs, thick TBCs (4 mm), and TBCs with unique compositions.

Future work with the SPPS process to create TBCs includes additional exploration and fabrication of ultra low-thermal conductivity coatings, combining compositional engineering (rare earth compositions) with microstructural engineering (porosity layering). The fabrication of thick coatings by SPPS, already demonstrated, is being explored to create practical components such as abradable outer air seals. Also, by manipulation of process parameters, it is possible to fabricate hard, dense, and crack free coatings by the SPPS process (Fig. 13) with numerous applications. Additional descriptions of these coatings can be found in Ref 16 and in publications still under review.

And finally, there is much to be learned in the area of fundamental understanding of many aspects to the SPPS process, including a better understanding of droplet

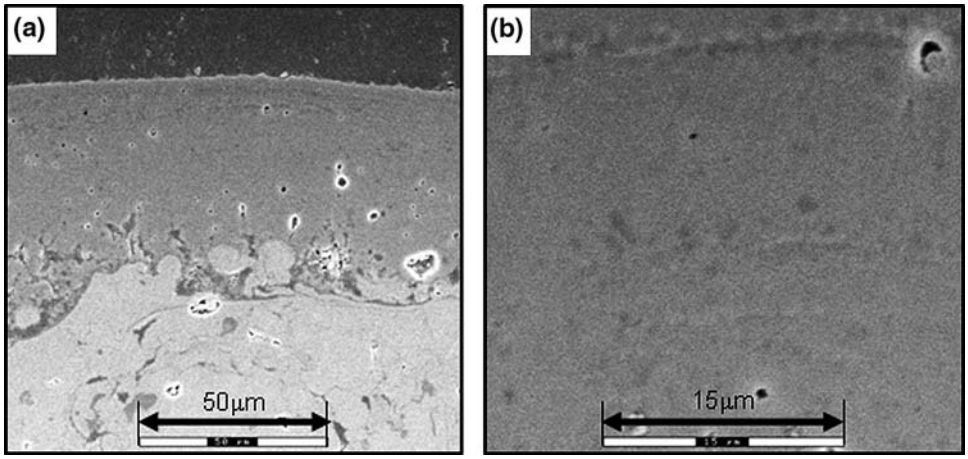

Fig. 13 Micrograph of 95% dense alumin-YSZ coating deposited by SPPS. (a) Low magnification and (b) higher magnification

breakup and the chemical and physical changes that result from heating.

Acknowledgments

This work was supported by the U.S. Office of Naval Research under Grant N000014-02-1-0171 managed by Drs. Lawrence Kabacoff and Steven Fishman, by the U.S. Office of Naval Research under Grant No. N00014-04-M-0316 managed by Mr. Lewis R. Schmidt, and by the U.S. Department of Energy (DoE) Office of Fossil Energy National Energy Technology Laboratory under Grant No. 03-01-SR107. Special thanks to Peter Strutt, Danny Xiao and Paul Bryant of Inframat Corp., and Mark Aindow, Peter Bonzani, Saptarshi Basu, Fang Wu, and Alper Ozturk of UConn for fruitful discussion and advice.

References

1. P. Fauchais, G. Montavon, M. Vardelle, and J. Cedelle, Developments in Direct Current Plasma Spraying, *Surf. Coat. Technol.*, 2006, **201**(5), p 1908-1921
2. E. Bouyer, F. Gitzhofer, and M.I. Boulos, *Progress in Plasma Processing of Materials*, P. Fauchais, Ed., Begell House, NY, USA, 1997, p 735-750
3. F. Gitzhofer, M.-E. Bonneau, and M. Boulos, *Thermal Spray 2001: New Surfaces For A New Millennium*, C.C. Berndt, K.A. Khor, and E. Lugscheider, Eds., ASM International, Materials Park, OH, USA, 2001, p 61-68
4. P. Fauchais, V. Rat, C. Delbos, J.F. Coudert, T. Chartier, and L. Bianchi, Understanding of Suspension DC Plasma Spraying of Finely Structured Coatings for SOFC, *IEE Trans. Plasma Sci.*, 2005, **33**(2), p 920-930
5. A. Vasiliev, N.P. Padture, and X. Ma, Nanostructured Coatings of Metastable Ceramics: Part I, The ZrO_2-Al_2O_3 Binary System, *Acta Mater.*, 2006, **54**, p 4913-4920
6. A. Vasiliev and N.P. Padture, Nanostructured Coatings of Metastable Ceramics: Part II, The Ternary ZrO_2-Y_2O_3-Al_2O_3 System, *Acta Mater.*, 2006, **54**, p 4921-4928
7. J. Karthikeyan, C.C. Berndt, S. Reddy, J.-Y. Wang, A.H. King, and H. Herman, Nanomaterial Deposits Formed by DC Plasma Spraying of Liquid Feedstocks, *J. Am. Ceram. Soc.*, 1998, **81**, p 121-128
8. J. Karthikeyan, C.C. Berndt, J. Tikkanen, J.-Y. Wang, A.H. King, and H. Herman, Preparation of Nanophase Materials by Thermal Spray Processing of Liquid Precursors, *Nanostruct. Mater.*, 1997, **9**(1), p 137-140
9. J. Karthikeyan, C.C. Berndt, J. Tikkanen, J.-Y. Wang, A.H. King, and H. Herman, Nanomaterial Powders and Deposits Prepared by Flame Spray Processing of Liquid Precursors, *Nanostruct. Mater.*, 1997, **8**(1), p 61-71
10. N.P. Padture, K.W. Schlichting, T. Bhatia, A. Ozturk, B. Cetegen, E.H. Jordan, M. Gell, S. Jiang, T.D. Xiao, P.R. Strutt, E. Garcia, P. Miranzo, and M.I. Osendi, Towards Durable Thermal Barrier Coatings with Novel Microstructures Deposited by Solution Precursor Plasma Spray, *Acta Mater.*, 2001, **49**, p 2251-2257
11. S.D. Parukuttyamma, J. Margolis, H. Liu, C.P. Grey, S. Sampath, H. Herman, and J.B. Parise, Yttrium Aluminum Garnet (YAG) Films Through a Precursor Plasma Spraying Technique, *J. Am. Ceram. Soc.*, 2001, **84**(8), p 1906-1908
12. E. Bouyer, G. Schiller, M. Muller, and R.H. Heane, Thermal Plasma Chemical Vapor Deposition of Si-Based Ceramic Coatings from Liquid Precursors, *Plasma Chem. Plasma Process.*, 2001, **21**(4), p 523-546
13. T. Bhatia, A. Ozturk, L. Xie, E. Jordan, B. Cetegen, M. Gell X. Ma, and N. Padture, Mechanisms of Ceramic Coating Deposition in Solution Precursor Spray, *J. Mater. Res.*, 2001, **17**(9), p 2363-2372
14. N.P. Padture, M. Gell, and E.H. Jordan, Thermal Barrier Coatings for Gas-Turbine Engine Applications, *Science*, 2002, **296**, p 280-285
15. L. Xie, X. Ma, E.H. Jordan, N.P. Padture, T.D. Xiao, and M. Gell, Identification of Coating Deposition Mechanisms in the Solution-Precursor Plasma-Spray Process using Model Spray Experiments, *Mater. Sci. Eng. A*, 2003, **362**, p 204-212
16. X.Q. Ma, J. Roth, T.D. Xiao, and M. Gell, Eds., Study of Unique Microstructure in SPS Ceramic Nanocoatings, *Thermal Spray 2003: Advancing the Science and Applying the Technology*, Vol. 2, May 5-8, 2003 (Orlando, FL), ASM International, 2003, p 1471-1476
17. X.Q. Ma, T.D. Xiao, J. Roth, L.D. Xie, E.H. Jordan, N.P. Padture, M. Gell, X.Q. Chen, and J.R. Price, Thick Thermal Barrier Coatings with Controlled Microstructures Using Solution Precursor Plasma Spray Process, *Thermal Spray 2004: Advances in Technology and Application*, ASM International, May 10-12, 2004 (Osaka, Japan), ASM International, 2004
18. A. Ozturk and B.M. Cetegen, Modeling of Plasma Assisted Formation of Precipitates in Zirconium Containing Liquid Precursor Droplets, *Mater. Sci. Eng. A*, 2004, **384**, p 331-351
19. X. Ma, F. Wu, J. Roth, M. Gell, and E. Jordan, Low Thermal Conductivity Thermal Barrier Coating Deposited by the Solution

Plasma Spray Process, *Surf. Coat. Technol.*, 2006, **201**, p 3343-3349
20. L. Xie, D. Chen, E.H. Jordan, A. Ozturk, F. Wu, X. Ma, B.M. Cetegen, and M. Gell, Formation of Vertical Cracks in Solution- Precursor Plasma-Sprayed Thermal Barrier Coatings, *Surf. Coat. Technol.*, 2006, **201**, p 1058-1064
21. L. Xie, E.H. Jordan, and M. Gell, Phase and Microstructural Stability of Precursor Plasma Sprayed Thermal Barrier Coatings, *Mater. Sci. Eng. A*, 2004, **381**, p 189-195
22. M. Gell, L. Xie, E. H. Jordan, and N. Padture, Mechanisms of Spallation of Solution Precursor Plasma Spray Thermal Barrier Coatings, *Surf. Coat. Technol.*, 2004, **188-189**, p 101-106
23. M. Madhwal, E.H. Jordan, and M. Gell, Failure Mechanisms of Dense Vertically Cracked Thermal Barrier Coatings, *Mater. Sci. Eng. A*, 2004, **384**, p 151-161
24. L. Xie, X. Ma, A. Ozturk, E.H. Jordan, N.P. Padture B.M. Cetegen, D.T. Xiao, and M. Gell, The Effects of Processing Parameters on the Spray Patterns Produced in the Solution Precursor Plasma Spray of Thermal Barrier Coatings, *Surf. Coat. Technol.*, 2004, **183**(1), p 51-61
25. E.H. Jordan, L. Xie, C. Ma, M. Gell, N. Padture, B. Cetegen J. Roth, T.D. Xiao, and P.E.C. Bryant, Superior Thermal Barrier Coatings Using Solution Precursor Plasma Spray, *J. Therm. Spray*, 2004, **13**(1), p 57-65
26. L. Xie, X. Ma, E.H. Jordan, N.P. Padture, T.D. Xiao, and M. Gell, Deposition of Thermal Barrier Coatings Using Solution Precursor Plasma Spray Process, *J. Mater. Sci.*, 2004, **39**, p 1639-1636
27. L. Xie, X. Ma, E.H. Jordan, N.P. Padture, T.D. Xiao, and M. Gell, Highly Durable Thermal Barrier Coatings Made by the Solution Precursor Plasma Spray Process, *Surf. Coat. Technol.*, 2004, **177-178**, p 97-102
28. A. Jadhav, N. Padture, F. Wu, E. Jordan, and M. Gell, Thick Ceramic Thermal Barrier Coatings with High Durability Deposited Using Solution-Precursor Plasma Spray, *Mater. Sci. Eng. A*, 2005, **405**, p 313-320
29. M. Gell, F. Wu, E.H. Jordan, N.P. Padture, B.M. Cetegen, L. Zie, A. Ozturk, E. Cao, A. Jadhav, D. Chen, and X. Ma, The Solution Precursor Plasma Spray Process for Making Highly Durable Thermal Barrier Coatings, *Proceedings of GT2005, ASME Turbo Expo 2005*
30. A. Ozturk and B.M. Cetegen, Experiments on Ceramic Formation from Liquid Precursor Spray Axially Injected into an Oxy-acetylene Flame, *Acta Mater.*, 2005, **53**, p 5203-5211
31. A. Ozturk and B.M. Cetegen, Modeling of Axially and Transversely Injected Precursor Droplets into a Plasma Environment, *Int. J. Heat Mass Trans.*, 2005, **48**(21-22), p 4367-4383
32. A. Ozturk and B.M. Cetegen, Morphology of Ceramic Particulates Formed in a Premixed Oxygen/Acetylene Flame from Mono-size Liquid Precursor Droplets, *Acta Mater.*, 2005, **53**, p 2531-2544
33. S. Basu and B.M. Cetegen, Modeling of Thermo-physical Processes in Liquid Ceramic Precursor Droplets Injected into a Plasma Jet, *Int. J. Heat Mass Trans.*, 2007, **50**(17-18), p 3278-3290
34. A. Ozturk and B.M. Cetegen, Modeling of Axial Injection of Ceramic Precursor Droplets into an Oxy-Acetylene Flame Environment, *Mater. Sci. Eng. A*, 2006, **422**(1-2), p 163-175
35. D. Chen, Unpublished research, University of Connecticut, 2007
36. X. Ma, F. Wu, Jeff Roth, Maurice Gell, and E.H. Jordan, Low Thermal Conductivity Thermal Barrier Coating Deposited by the Solution Plasma Spray Process, *Surf. Coat. Technol.*, 2006, **201**, p 4447-4452
37. A.G. Evans, D.R. Mumm, J.W. Hutchinson, G.H. Meier, and F.S. Pettit, Mechanisms Controlling the Durability of Thermal Barrier Coatings, *Progr. Mater. Sci.*, 2001, **46**, p 505-553
38. C. Moreau, J.F. Bisson, R.S. Lima, and B.R. Marple, Diagnostics for Advanced Materials Processing by Plasma Spraying, *Pure Appl. Chem.*, 2001, **77**(2), p 443-462
39. R.R. Chamberlin and J.S. Skarman, Chemical Spray Deposition for Inorganic Films, *J. Electrochem. Soc.*, 1966, **113**, p 86-89
40. G.L. Messing, S.-C. Zhang, and G.V. Jayanthi, Ceramic Powder Synthesis by Spray Pyrolysis, *J. Am. Ceram. Soc.*, 1993, **76**(11), p 2707-2726
41. S.E. Pratsinis, Flame Aerosol Synthesis of Ceramic Powders, *Progr. Energy Combust. Sci.*, 1998, **24**(3), p 197-219
42. P.S. Patil, Versatility of Spray Pyrolysis Technique, *Mater. Chem. Phys.*, 1999, **59**, p 185-198
43. R.M. Laine, R. Baranwal, T. Hinklin, D. Treadwell, A. Sutorik, C. Bickmore, K. Waldner, and S.S. Neo, Making Nanosized Oxide Powders from Precursors by Flame Spray Pyrolysis, *Key. Eng. Mat.*, 1999, **159**(1), p 17-24
44. T.A. Taylor, U.S. Patent no. 5,073,433, 1991